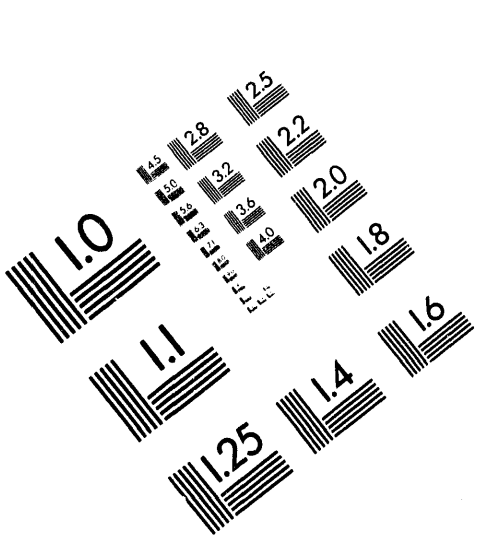

Association for Information and Image Management
1100 Wayne Avenue, Suite 1100
Silver Spring, Maryland 20910
301/587-8202

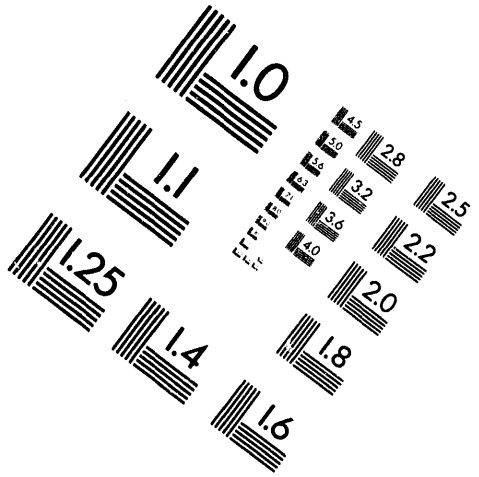

Centimeter

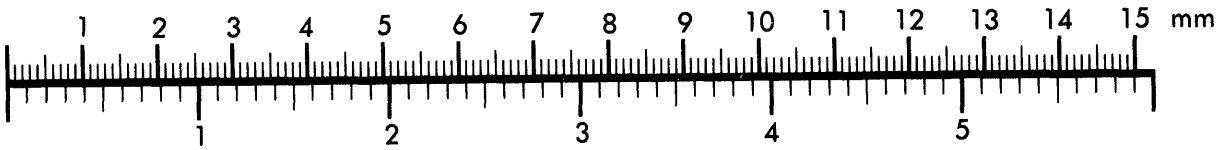

Inches

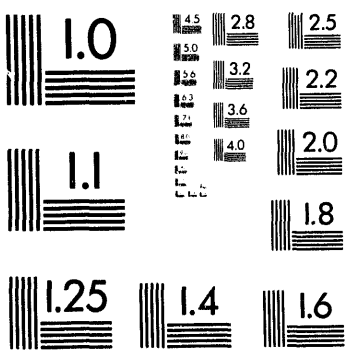

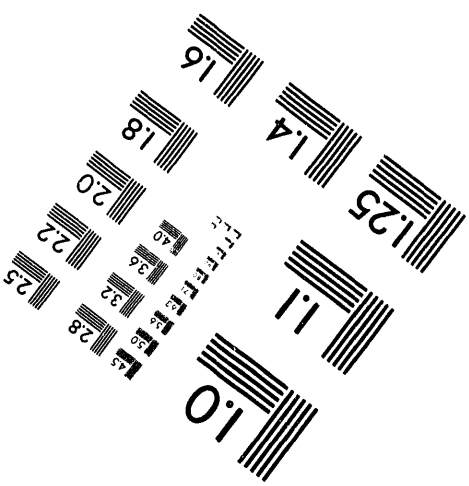

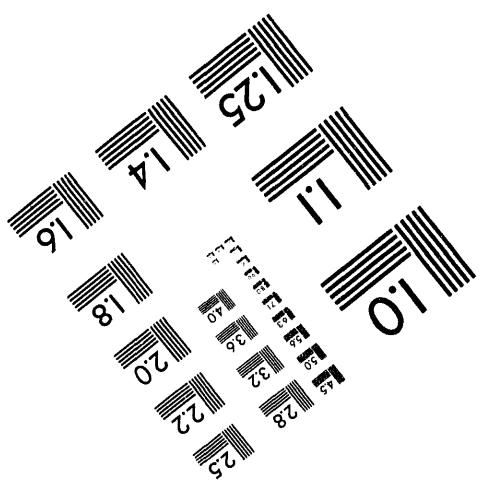

MANUFACTURED TO AIIM STANDARDS
BY APPLIED IMAGE, INC.

1 of 1

PLASMA ELECTRODE POCKELS CELLS FOR THE BEAMLET AND NIF LASERS

Mark A. Rhodes, B. Woods, J. DeYoreo, J. Atherton
University of California
Lawrence Livermore National Laboratory, PO Box 808 L-490
Livermore, CA 94550
510-422-9114

ABSTRACT

We describe Plasma Electrode Pockels Cells (PEPC) for the Beamlet laser and the proposed National Ignition Facility (NIF) laser. These PEPCs, together with passive polarizers, function as large aperture (>35 × 35 cm^2) optical switches enabling the design of high-energy (>5 kJ), multipass laser amplifiers. In a PEPC, plasma discharges form on both sides of a thin (1 cm) electro-optic crystal (KDP). These plasma discharges produce highly conductive and transparent electrodes that facilitate rapid (<100 ns) and uniform charging of the KDP up to the half-wave voltage (17 kV) and back to zero volts.

We discuss the operating principles, design, and optical performance of the Beamlet PEPC and briefly discuss our plans to extend PEPC technology for the NIF.

I. INTRODUCTION

Studies on the design of high-energy laser drivers for inertial confinement fusion (ICF) experiments[1] show that a multipass amplifier architecture offers a significant cost savings over designs based on single-pass amplifiers. One straightforward design of a multipass amplifier is to use an optical switch to trap an optical pulse within a laser cavity and then to divert the pulse out of the cavity after it reaches the required energy. Figure 1 illustrates this concept where the switch is comprised of a Pockels Cell and a passive polarizer. By rotating the polarization of the beam, the Pockels cell controls whether the beam is transmitted through or reflected from the polarizer.

High-energy lasers for ICF experiments are typically designed with large apertures (>30 cm) to keep the fluence below the damage threshold for the various optical components. Until recently, there was no optical switch technology that could be scaled to the apertures required for the next generation of ICF drivers. In conventional Pockels cells, a longitudinal electric field is applied to an electro-optic crystal via external ring-electrodes. To achieve a reasonably uniform field distribution in the crystal, the crystal aspect ratio (diameter/length) must be no greater than 1:1(1:2 is desirable). Since the required aperture in high-energy ICF drivers is on the order of 40 cm, the thickness, and therefore the optical path length through the crystal, would be >40 cm. A crystal this thick would have excessive optical absorption, strain depolarization, and cost. An alternate Pockels cell design approach, which allows for thin crystals, employs transparent, conductive thin films applied to the crystal surfaces. This approach is also not suitable for ICF lasers because such films will damage at the optical fluence (up to 11 J/cm^2) produced in these lasers.

We have developed an efficient and reliable optical switch technology that does scale to the required apertures for ICF lasers and allows arbitrary aperture shape. This switch is based on a PEPC. The PEPC, originally invented at Lawrence Livermore National Laboratory in the mid 1980's,[2] has been incorporated into the Beamlet laser which recently met a major milestone by producing a 5.5-kJ, 3-ns output pulse.[3] In this paper, we discuss the design, operation, and performance of the Beamlet PEPC. In addition, we discuss our plan to scale PEPC technology for use in the proposed NIF.[4]

Figure 1. An optical switch enables a multipass laser amplifier architecture. The switch deflects the optical pulse out of the cavity after multiple gain passes.

II. THE PLASMA-ELECTRODE POCKELS CELL CONCEPT

Figure 2 shows a top view cross-section of a PEPC and a simplified schematic of the required external electronic circuit. Plasma discharges formed on each side of the KDP crystal act as highly conductive and transparent electrodes. Voltage from the switch-pulse generator is applied to the KDP via these plasma electrodes. As in a conventional Pockels cell, if the voltage across the crystal is V_π, the half-wave voltage (17 kV for KDP), the polarization of an incoming linearly-polarized beam is rotated by 90°.

Requirements on the plasma and switch-pulse generators flow down from the switching speed requirement placed on the PEPC. In the Beamlet laser, the optical pulse propagates through the cavity for two round-trips leading to four passes through the amplifier. The polarizer is arranged so that when no voltage is applied to the PEPC crystal, the cavity is open while the cavity is closed when the crystal is charged to V_π. To switch the optical pulse out of the cavity, the PEPC must be able to change state in less than the cavity round-trip transit-time, which is about 240 ns for Beamlet. We chose 100 ns as the nominal switching speed to allow extra time for voltage equilibration across the crystal aperture. The time constant by which the voltage on the crystal changes is given by $\tau = Z_{sw}C_{kdp}$, where Z_{sw} is the output impedance of the switch pulser and C_{kdp} is the capacitance of the KDP crystal. Since the relative dielectric constant, ε_r, for KDP is 20 and the Beamlet KDP crystal is 37 × 37 cm^2 and 1 cm thick, C_{kdp}=2500 pF. It takes four time constants to charge the crystal to 98% of V_π. So τ must be one-fourth of our desired switching speed or 25 ns. This implies that Z_{sw} must be 10 Ω. This sets the peak current that must be delivered by the switch-pulse generator $I_{sw} = V_\pi / Z_{sw}$ = 1.7 kA. The plasma current, I_p, at the time the switch-pulse is fired must be > I_{sw} otherwise the current from the switch-pulser charging the crystal clamps at I_p, which increases the time required to fully charge the crystal.[5] This effect is due to the diode nature of the plasma discharge. Figure 2 depicts the plasma current and the switch-pulse current with thick arrows. On side 2, the plasma and switch-pulse currents are in the same direction; on side 1 they are in opposite direction, so they tend to cancel. If the peak switch-pulse current is greater than the plasma current, the current at the side 1 anode must go negative, which means that it is emitting electrons. This cannot happen on the time scale of the switch pulse.

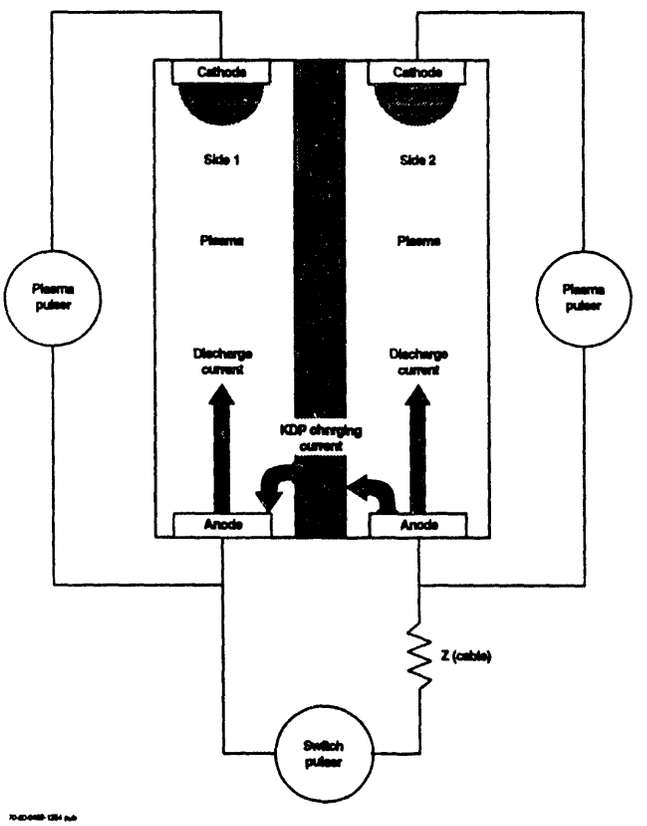

Figure 2. A cross-sectional view of a PEPC showing the required external electronic circuit. The plasma pulsers produce the plasma-electrodes while the switch pulser applies voltage across the KDP crystal.

III. DESIGN OF THE BEAMLET PEPC

Figures 3(a) and 3(b) are photographs of the Beamlet PEPC. Figure 3(a) shows a full view of the Beamlet PEPC; Figure 3(b) shows the Beamlet PEPC fully integrated into the Beamlet. In this section we describe design details for the PEPC and its associated subsystems including: the PEPC assembly, the vacuum and gas supply system, the discharge electrodes, the plasma-pulser, and the switch-pulser.

A. PEPC Assembly

Figure 4 shows an exploded diagram of the PEPC assembly. The KDP crystal, potted into a ceramic midplane, is in the center between two housings which are in turn sandwiched between a pair of fused silica windows. The housings define the vacuum regions on each side of the crystal. The cell bodies also hold the discharge electrodes in place and interface to the vacuum pumping system. The fused silica windows seal the vacuum regions on the outside and allow transmission of the optical pulse. The windows and the KDP crystal are antireflection (A/R) coated with sol-gel. To minimize etalon effects, the windows and the KDP crystal are wedged. In addition, the windows are

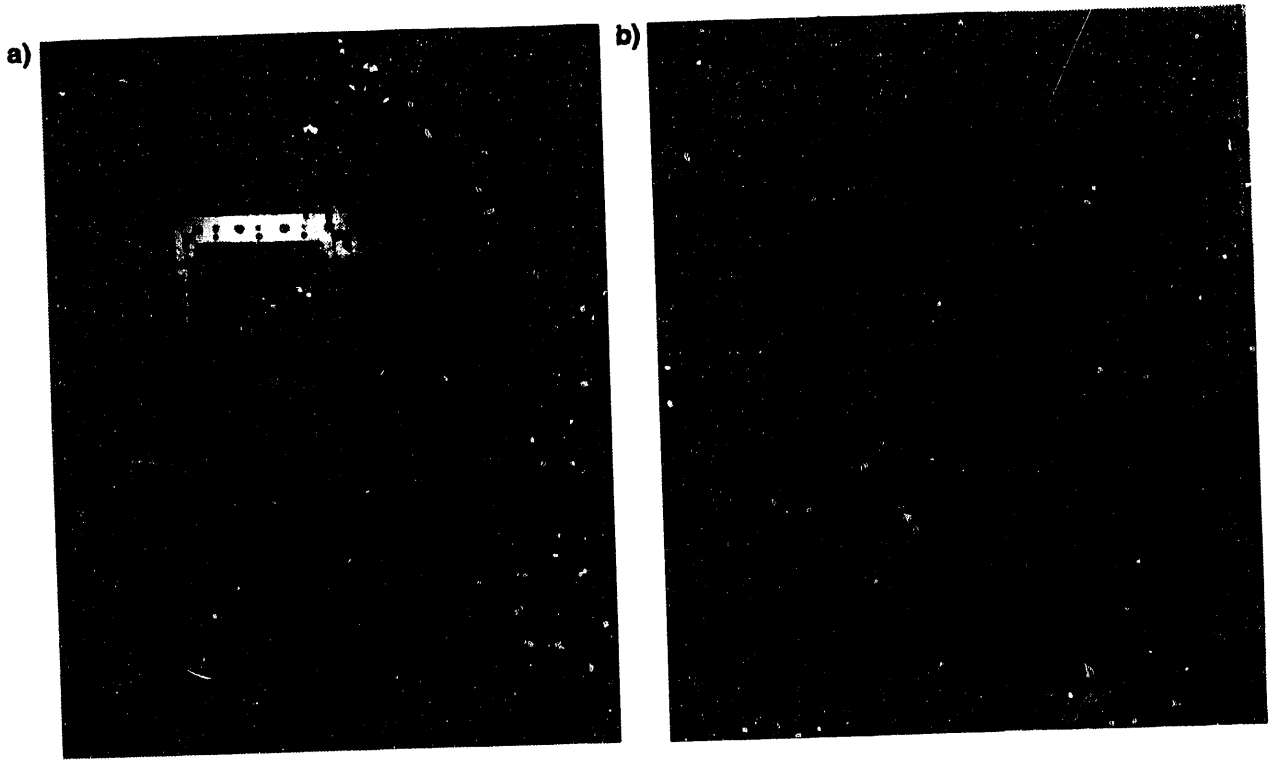

70-50-0494-1845 pub

Figure 3. a) Photograph of the Beamlet PEPC before installation into the Beamlet laser. b) Photograph of the Beamlet PEPC fully integrated into the Beamlet laser.

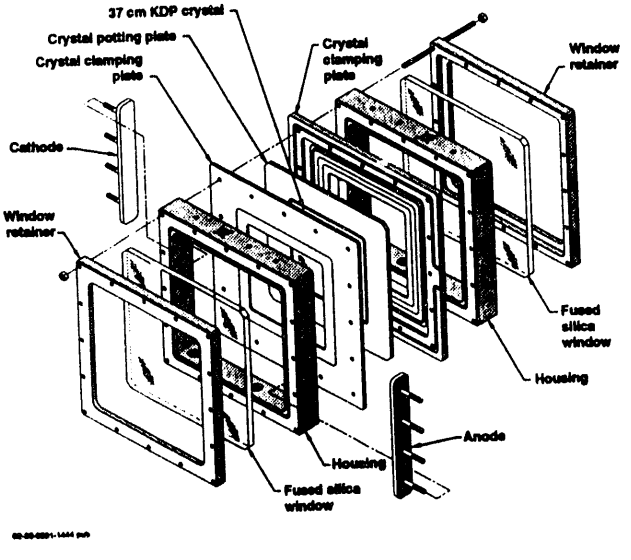

Figure 4. Exploded diagram of the PEPC assembly showing the sandwich structure.

mounted at a slight angle to keep reflections from returning to the amplifier through the spatial-filter pin-hole plane.

The housing assembly sits on top of a support structure. The support structure provides adjustment of tip, tilt, and twist so that the PEPC may be properly aligned in the Beamlet cavity. The support structure also holds the vacuum pumping system.

B. Vacuum and Gas System

The vacuum and gas system provides the required environment inside the PEPC for optimum formation of the plasma electrodes. A two-stage turbomolecular pump evacuates the PEPC interio to $<5 \times 10^{-5}$ torr. This base pressure insures that the concentration of impurity species in the plasma is low enough to not degrade the discharge uniformity. The gas system injects the working gas, a mixture of helium plus 1% oxygen, into the cell and maintains the gas pressure at 35 mtorr with active feedback control. The feedback system uses a capacitance manometer to monitor the cell pressure and drives a servo loop actuating

a gas metering valve. The operating pressure is maintained by flowing gas while the turbo pump continuously evacuates the cell.

C. Discharge Electrodes

The plasma electrodes are formed by driving current between pairs of anodes and cathodes. The anodes are simple bars of stainless steel. The cathodes however are planar magnetron structures as shown in Figure 5. Permanent magnets beneath the cathode surface provide a closed E × B path for electron flow on the cathode surface leading to enhanced plasma density near the cathode. Compared to an ordinary cold cathode, the magnetron cathodes result in lower operating pressure and lower voltage across the anode-cathode gap.

During the discharge, electrons are emitted from the cathode by bombardment from helium ions accelerated toward the cathode by the discharge potential. However, this ion bombardment also leads to sputtering of the cathode material. We found that this sputtered material can deposit on the crystal and window surfaces leading to a degradation in the optical damage threshold. To eliminate this deposition, the cathode surfaces are made from high purity graphite so the sputtered material is carbon. The sputtered carbon reacts with the 1% oxygen in the plasma to form CO and CO_2,which is pumped away by the vacuum system. With this process, we have found no plasma-caused degradation of the optical surfaces in tests up to 80,000 shots.

D. Plasma-Pulser

Figure 6 shows a simplified schematic of the plasma-pulser. The plasma is initiated by a high-voltage, low-current power supply which provides enough voltage to breakdown the gas (about 1.5 kV) and then provides a constant discharge current of 30 mA. The voltage required to maintain this "simmer" discharge is about 300 V. We found that power dissipated at the cathode leads to cathode heating (about 9°C). The heated cathode causes radiative heating of the crystal near the cathode (about 2°C). The thermal gradient in the crystal produces strain that increases beam depolarization near the cathode. To minimize this heating and the associated reduction in switching efficiency, we gate the simmer discharge on for about 500 ms before the high-current pulse. Gating the simmer current minimizes the average power dissipated at the cathode. The high-current pulse is produced by discharging a 5 μF capacitor charged from 4–7 kV. Figure 7 shows a typical current waveform and the relative timing of the switch-pulse.

E. Switch-Pulser

The switch-pulser[6] produces a nominally rectangular pulse that is applied across the KDP crystal via the plasma electrodes. The switch-pulser satisfies several important requirements: jitter from shot to shot is <2 ns, a voltage flat-top at least 50 ns long is within ±2% of V_π, and after the pulse, the voltage returns to zero ±2% of V_π so that the optical pulse is efficiently switched out of the cavity. Figure 8 is a schematic of the switch pulser. The rectangu-

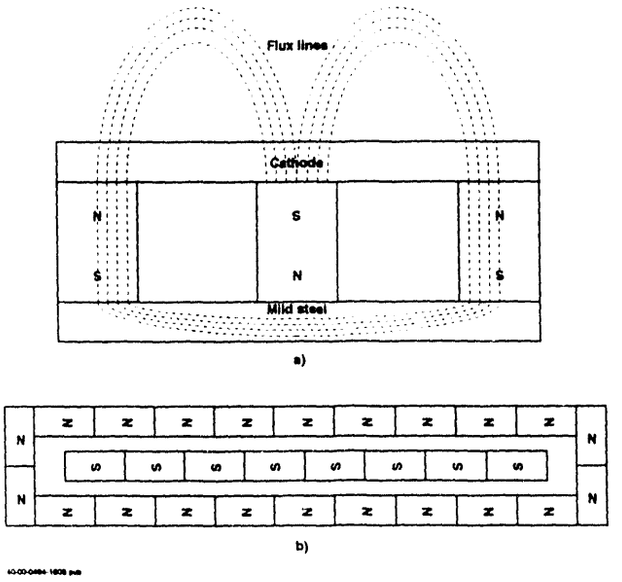

Figure 5. a) Side view and b) magnet layout for the planar magnetron cathodes used in the PEPC. The magnetron cathodes provide a uniform discharge without thermionic emission.

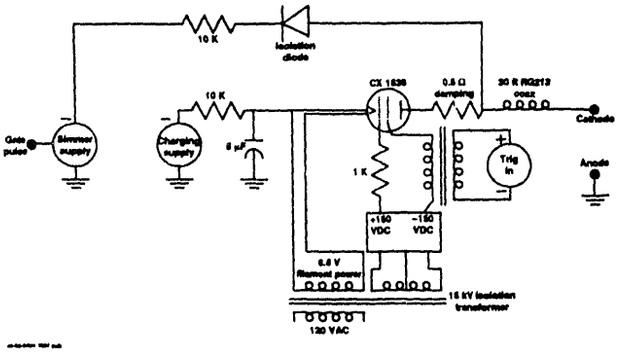

Figure 6. Schematic diagram the of the plasma-pulse generator. A thyratron switches a charged capacitor across the discharge electrodes to produce a plasma current up to 5 kA.

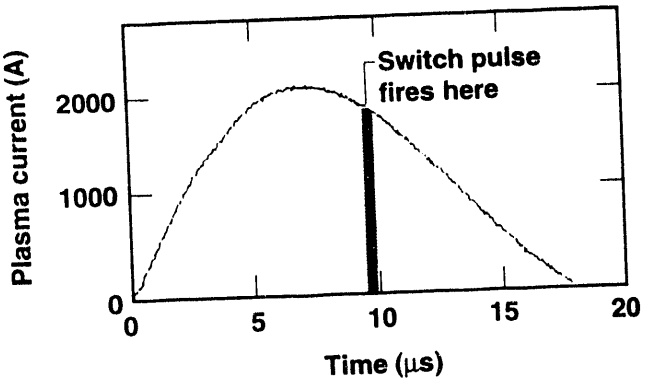

70-50-0594-2403 pub

Figure 7. Waveform of the plasma current for a 2-kA pulse and the relative timing of the switch-pulse.

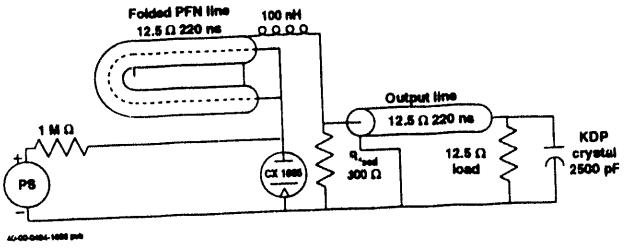

Figure 8. Schematic diagram of the switch-pulse generator. Sections of coaxial cable act as a pulse forming network (PFN) to produce a nominally rectangular pulse shape. Multiple cables are connected in parallel to achieve the low impedance required to charge the 2500 pF capacitive load of the KDP crystal in <100 ns.

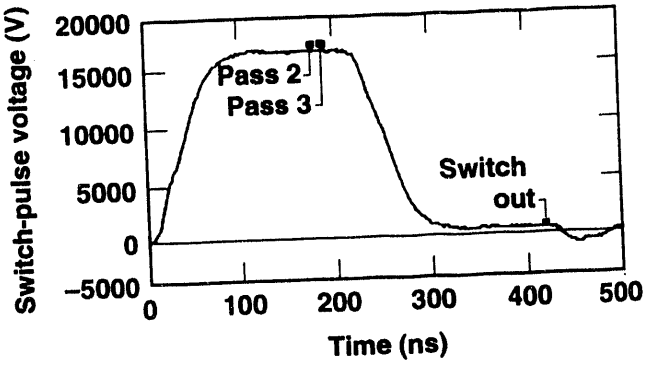

70-50-0594-2402 pub

Figure 9. Voltage waveform across the PEPC during normal operation and the times when the optical pulse traverses the cell (twice when the voltage is on and once after the cell is discharged).

lar pulse is produced by employing sections of coaxial cable as a pulse forming network (PFN). A high-voltage power supply charges the PFN to twice the required output voltage and a thyratron switches the charged PFN into the output line which is also comprised of coaxial cable sections. Multiple PFN and output lines are connected in parallel to achieve the switch-pulser impedance required to charge and discharge the crystal in less than the cavity round trip transit time. As an example, the Beamlet switch-pulser uses four 50-Ω PFN and output lines in parallel to achieve a pulser impedance of 12.5 Ω. Figure 9 shows a typical waveform from the Beamlet switch-pulser. It illustrates the voltage pulse and the relative timing of the optical pulse on the multiple passes through the cell.

IV. PEPC OPTICAL PERFORMANCE

Operation of the Beamlet PEPC as part of the Beamlet laser began in February 1994. Before operation at high optical fluence, we evaluated the switching performance at low fluence with the PEPC installed into the Beamlet laser cavity. Figure 10 shows a simplified diagram of the Beamlet laser. This experimental setup shows the beam from the front-end laser injected into the spatial filter. A small injection mirror (not shown) reflects the beam toward cavity mirror M_1, passing through the cavity amplifier (which was not energized for the low fluence tests). The beam reflects from M_1 and passes back through the amplifier and spatial filter before it illuminates the PEPC at full aperture (35 × 35 cm). After traversing the PEPC, the beam reflects from the polarizer if the PEPC is off and passes through the polarizer if the PEPC is on. A portion of the light transmitted by the polarizer also is transmitted by cavity mirror M_2. This beam is down-collimated by diagnostic lens L_3 and other small aperture optics (not shown). The image plane of the PEPC is focused onto a high-resolution CCD video camera. We take the ratio of switch-on and switch-off images to produce a switching efficiency image as shown in Figure 11. Switching efficiency includes losses due only to beam depolarization and does not include losses from surface reflections (<0.1% total for both windows and the crystal). Switching efficiency also does not include absorption which is about 5% for a 1-cm KDP crystal and negligible for the windows. For this low-fluence test, we observed an average switching efficiency across the aperture of 99.5% while the minimum was 97.5% in the upper left hand corner. The regions of lower switching efficiency in the corners are caused by strain induced depolarization in the fused silica windows from vacuum loading.

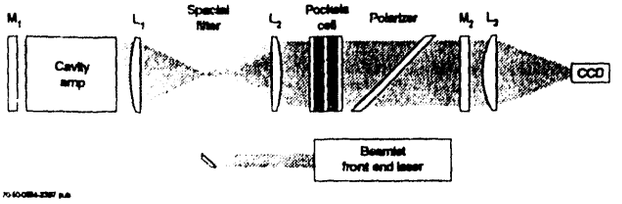

Figure 10. Simplified diagram of the Beamlet laser showing the experimental setup used for evaluating the switching performance of the PEPC at low fluence. An optical pulse from the Beamlet front-end laser propagates through the PEPC and polarizer. A high-resolution CCD video camera images the light transmitted by the PEPC-polarizer combination.

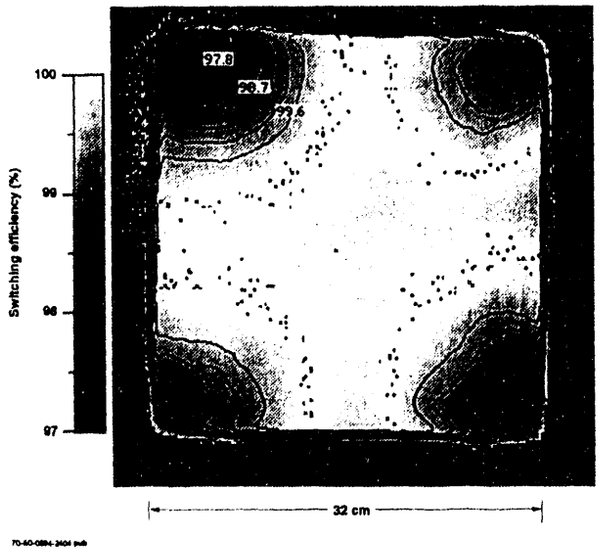

Figure 11. Image of the Beamlet PEPC showing switching efficiency across the aperture. Lower switching efficiency in the corners is due to strain induced birefringence in the silica windows from vacuum loading.

During a full system shot, the cavity amplifier is energized. The voltage pulse applied to the switch starts about the same time the optical pulse hits the injection mirror. While the optical pulse propagates towards mirror M_1 and the first two gain passes through the amplifier, the switch charges. The voltage across the crystal is fully equilibrated by the time the optical pulse reaches the PEPC which rotates the polarization 90° so it passes through the polarizer. The beam reflects from mirror M_2, passes through the polarizer and rotates another 90° by the PEPC before it propagates back toward the amplifier for two more gain passes. During this 240-ns interval, the voltage across the PEPC discharges. When the pulse returns again, the beam is not rotated so it reflects off the polarizer and out of the cavity. While details of the Beamlet laser performance[3] are not within the scope of this paper, the main Beamlet cavity has so far produced up to 6 kJ in a 3-ns pulse with switched, four-pass operation. During these tests, the Beamlet PEPC operated reliably and reproducibly exhibiting high-fluence (average of 5 J/cm^2) switching efficiency >99.5 % for both cavity closed and cavity open states.

V. PEPC FOR THE NATIONAL IGNITION FACILITY

The NIF[4] is a proposed 1.8-MJ ICF facility. The NIF laser is based on technology demonstrated with the Beamlet laser including a four-pass amplifier cavity with active PEPC switching. We are extending PEPC technology to produce a device suitable for use in the NIF. The baseline NIF laser design consists of 192 individual beamlets packed into arrays 4 high by 12 wide. All the optical components in the NIF laser cavity, including the PEPCs, must be arranged in closely packed 4 × 12 arrays. The 4 × 12 PEPC array, shown in Figure 12, will be comprised of 1 × 4 PEPC subassemblies shown in Figure 13. However, each 1 × 4 subassembly will be comprised of two independent 1 × 2 electrical modules shown schematically in Figure 14. In a 1 × 2 PEPC module, each plasma-pulser must produce a discharge that covers two crystals and each switch-pulser must charge two crystals. This de-

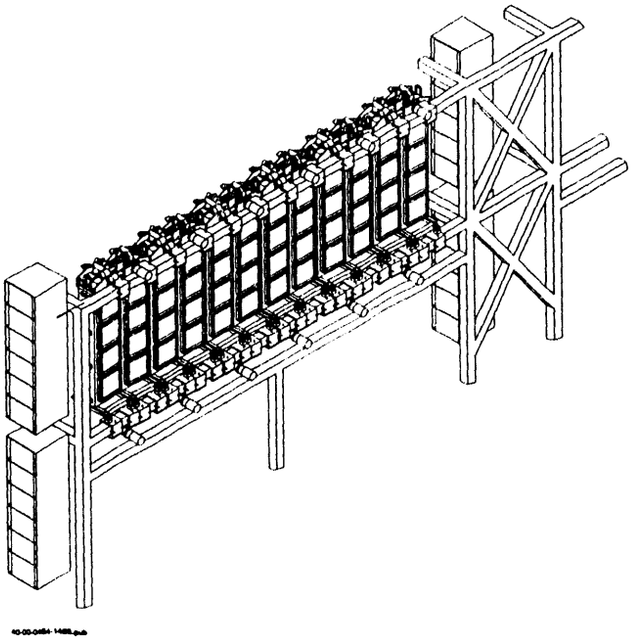

Figure 12. Conceptual design of a 4 × 12 PEPC array for the NIF.

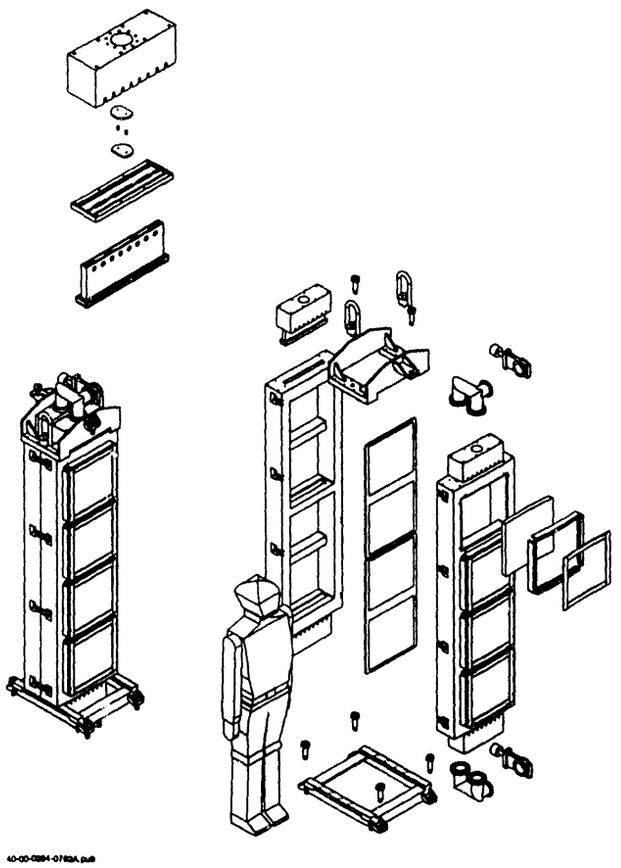

Figure 13. A 4 × 12 NIF PEPC array is comprised of twelve of these 1 × 4 PEPC building blocks.

sign allows all electrical and vacuum connections to be located along the top and bottom of a 4 × 12 array where they will not interfere will the optical beams. This design also minimizes the inter-beam spacing allowing the PEPC spacing to match that of other components in the cavity, the amplifiers in particular.

VI. CONCLUSION

We have discussed the technology of Plasma-Electrode Pockels Cells where plasma discharges facilitate uniform application of voltage to large-aperture, thin electro-optic KDP crystals. PEPC technology enables the construction of large-aperture optical switches for use in high-energy ICF laser drivers. Such a switch has been successfully incorporated into the design of the high-energy Beamlet laser where it switches a 5–6-kJ, 3-ns optical pulse out of the amplifier cavity after four gain passes. The Beamlet PEPC has demonstrated switching efficiency >99.5% and has operated reliably during Beamlet experiments.

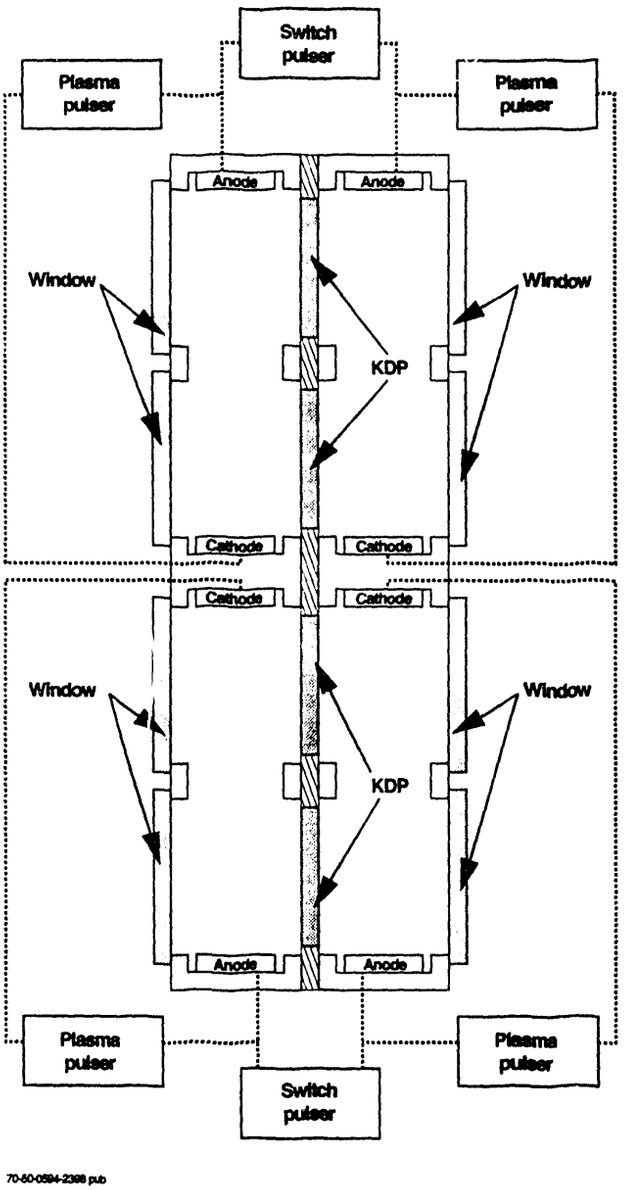

Figure 14. Each 1 × 4 NIF PEPC building block will be comprised of a pair of electrically independent 1 × 2 PEPCs. In a 1 × 2 module, the plasma discharge must span two crystals compared to one crystal in the Beamlet PEPC

We are scaling PEPC technology for use in the NIF laser. The NIF PEPC will be based on 1 × 2 electrical modules arranged in closely packed 4 × 12 arrays.

This work was performed under the auspices of the US Department of Energy by Lawrence Livermore National Laboratory under the contract number W-7405-ENG-48.

REFERENCES

1. J.R. Murray, J.H. Campbell, D.N. Frank, J.T. Hunt, and J.B. Trenholme, "The Nova Upgrade Beamlet Demonstration Project," *ICF Quarterly Report*, 1 (3), 89-107, Lawrence Livermore National Laboratory, Livermore, CA, UCRL-LR-105821-91-3 (1991).

2. J. Goldhar and M.A. Henesian, "Large-Aperture Electro-Optical Switches with Plasma Electrodes," *IEEE J. Quantum Electronics* **QE-22**, 1137 (1986).

3. Bruno M. Van Wonterghem, John R. Murray, D. Ralph Speck, and John H. Campbell, "Performance of the NIF Prototype Beamlet," *Eleventh Topical Meeting on the Technology of Fusion Energy*, New Orleans, LA, 1994.

4. "NIF Conceptual Design Report," Lawrence Livermore National Laboratory, Livermore, CA, UCRL-PROP-117093 (1994).

5. M. A. Rhodes, "Physical Processes Involved in the Operation of Very-Large-Aperture Pockels Cells Employing Plasma Electrodes," Lawrence Livermore National Laboratory, Livermore, CA, UCRL-JC-109595 (1992).

6. M. A. Rhodes and J. Taylor, "Pulse Power Requirements for Large-Aperture Optical Switches Based on Plasma-Electrode Pockels Cells," *Twentieth Power Modulator Symposium*, **IEEE CH3180-7**, 380 (1992).

DATE
FILMED
10/4/94

END